

Spatial distribution of pico- and nano-phytoplankton and bacteria in the Chukchi Sea in relation to water masses

ZHANG Fang^{1*}, HE Jianfeng¹, LIN Ling¹, LIU Ying^{1,2}, WANG Xiaoying^{1,3} & DING Chen⁴

¹ SOA Key Laboratory for Polar Science, Polar Research Institute of China, Shanghai 200136, China;

² College of Food Science & Technology, Shanghai Ocean University, Shanghai 201306, China;

³ College of Fisheries and Life Science, Shanghai Ocean University, Shanghai 201306, China;

⁴ Zhile Yingcai Education Center, Beijing 100022, China

Received 14 September 2012; accepted 11 November 2012

Abstract We evaluated the relationships between water masses and pico- and nano-phytoplankton and bacterial abundance in the Chukchi Sea. The abundance of picoplankton ranged from 0.01×10^3 cells·mL⁻¹ (100 m, station R05) to 2.21×10^3 cells·mL⁻¹ (10 m, station R05) and that of nanoplankton ranged from 0.03×10^3 cells·mL⁻¹ (100 m, station R07) to 2.21×10^4 cells·mL⁻¹ (10 m, station R05). The lowest abundance of bacteria in the whole water column (0.21×10^6 cells·mL⁻¹) was at 100 m at station R17, and the highest (9.61×10^6 cells·mL⁻¹) was at 10 m at station R09. Melting sea ice affected the physical characteristics of the Chukchi Sea by reducing salinity of the surface mixed layer, resulting in greater hydrodynamic stability of the water column. These changes were accompanied by increased bacterial abundance. The warm Pacific water brought nutrients into the Chukchi Sea, resulting in greater abundance of bacteria and nano-phytoplankton in the Chukchi Sea than in other regions of the Arctic Ocean. However, the abundance of pico-phytoplankton, which was related to chlorophyll *a* concentration, was higher in Anadyr water than in the other two water masses. The structures of pico- and nanoplankton communities coupled with the water masses in the Chukchi Sea can serve as indicators of the inflow of warm Pacific water into the Chukchi Sea.

Keywords Arctic Ocean, Chukchi Sea, bacteria, pico-phytoplankton, nano-phytoplankton

Citation: Zhang F, He J F, Lin L, et al. Spatial distribution of pico- and nano-phytoplankton and bacteria in the Chukchi Sea in relation to water masses. *Adv Polar Sci*, 2012, 23: 237-243, doi: 10.3724/SP.J.1085.2012.00237

0 Introduction

The Chukchi Sea (latitudes 65°—75°N, longitude 170°W) is a strip at the edge of the Arctic Ocean. The mean depth of the Chukchi Sea is 88 m, with 56% of its area having a depth of less than 55 m, and the salinity is 24‰—33.5‰^[1]. It connects to the Bering Sea via Bering Strait at the south, to the East Siberian Sea via De Long Strait, and to the Beaufort Sea at the Point Barrow in the northeast. The water of the Chukchi Sea is mainly from the Pacific Ocean, Arctic Ocean, and East Siberian Sea^[2-3], and its water masses are characterized as shelf sea-modified water masses. The Bering Sea water, which has a higher temperature and high salinity, flows into the Chukchi Sea and

significantly influences the process of ice melting in summer^[4]. There are two water masses that enter the Chukchi Sea successively in summer: Anadyr water (AW) (low temperature, high salinity, high silicate content) and Bering Shelf water (BSW) (melted sea ice, high temperature, low salinity, and low silicate content)^[5].

Autotrophic pico-flagellates (APF, particle size <2 μm) and autotrophic nano-flagellates (ANF, particle size 2—20 μm) are the main components of biomass and the main contributors to primary productivity in the Arctic Ocean^[6-7]. Because of the effects of warm and nutrient-rich input water from the North Pacific Ocean, the Chukchi Sea is not only a high primary productivity area^[8-9], it is also very efficient in producing organic carbon sediment^[10-11]. APF and ANF are especially important for carbon holding in this ecosystem^[12]. Bacterioplankton are also very important in recycling matter in the Arctic Ocean^[13]. In the Chukchi Sea,

* Corresponding author (email: zhangfang@pric.gov.cn)

one-half of the dissolved organic matter(DOM) produced by phytoplankton is absorbed by heterotrophic bacteria^[10]. After the phytoplankton bloom in summer, the heterotrophic bacteria biomass can even exceed the phytoplankton biomass^[14].

There have been few studies on APF and ANF community structures. According to previous studies, the ANF (5—20 μm) community is dominated by *Chaetoceros*, *Thalassiosirales*, and *Phaeocystis* in spring and summer^[14-16] while the APF (2—5 μm) community is dominated by *Microcystis*^[13]. In this area, the total bacterial abundance (10^7 — 10^9 cells·L⁻¹) is greater than that in any other area in the Arctic Ocean^[10].

In this study, we determined the correlations between water masses and spatial distribution of APF, ANF, and bacterioplankton in the Chukchi Sea using statistical methods. The spatial distribution of APF, ANF, and bacterio-

plankton were determined during the third Chinese National Arctic Research Expedition (the 3rd CHINARE-Arctic, July to September, 2008) by sampling across a latitudinal transect (R), in the Chukchi Sea. This study is helpful to evaluate the potential influence of input water from the Pacific Ocean on biological communities in the Chukchi Sea.

1 Materials and methods

1.1 Sampling and processing

Samples were collected during the 3rd CHINARE-Arctic. Figure 1 shows the setting of transects and stations. The surveyed transect was generally parallel with 170°W. Station R07 was located at the leading shallow beach. Each station was divided into 4—7 depths for sampling. Details are shown in Table 1.

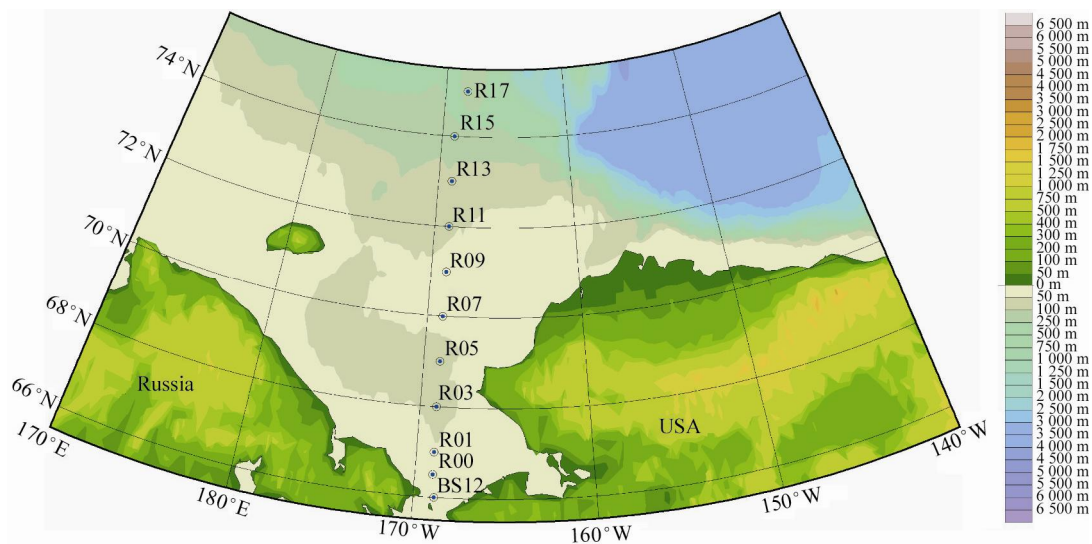


Figure 1 Map of Chukchi Sea showing location of sampling stations.

Table 1 Sampling information of R transect in the Chukchi Sea

| Stations | Latitude and Longitude | Depth/m | Sampling/m |
|----------|-------------------------|---------|----------------------|
| BS12 | 168°51.98'W, 65°59.99'N | 47.22 | 0/20/30/47 |
| R00 | 168°59.87'W, 66°30.00'N | 43.00 | 0/10/20/30/40/42 |
| R01 | 168°59.90'W, 66°59.70'N | 41.98 | 0/20/30/40 |
| R03 | 169°01.50'W, 67°59.70'N | 51.00 | 0/20/30/40/50 |
| R05 | 168°59.72'W, 68°59.70'N | 47.33 | 0/10/20/30/40/46 |
| R07 | 168°59.50'W, 69°59.70'N | 30.63 | 0/17/20/29 |
| R09 | 168°58.40'W, 70°59.6'N | 37.20 | 0/10/20/30 |
| R11 | 168°59.10'W, 71°59.87'N | 46.76 | 0/10/25/30/40 |
| R13 | 169°00.00'W, 73°00.00'N | 71.42 | 0/10/25/30/40 |
| R15 | 169°00.40'W, 73°59.50'N | 173.22 | 0/10/20/40/50/75/100 |
| R17 | 168°08.73'W, 75°00.09'N | 173.22 | 30/40/50/100 |

The temperature and salinity data at each station were acquired by a shipborne SBE 911 plus CTD (Sea-Bird

Electronics Inc., Washington, U.S.A.), and water samples at each level were collected using a 10-L Niskin water collector. Nutrient tests were performed *in situ* on the ship. Phosphate and nitrate were analyzed by a SKALAR SAN⁺⁺ nutrient automatic analyzer. Ammonium salts were determined by spectrophotometry as described by Li et al.^[17]. Chlorophyll *a* was tested by the extraction fluorescence method as follows: A 500 mL water sample was filtered through a Waterman GF/F glass fiber filter membrane, and then extracted with 90% acetone for 24 h at low temperature. The filtrate was tested using a Turner Designs Fluorometer 10-AU, and the amount of chlorophyll *a* was calculated as described by Parsons et al.^[18].

APF, ANF, and bacterial samples were collected as follows: 30—80 ml water was sampled from each level and fixed by adding pre-filtered formaldehyde solution (0.2 μm) to a final concentration of 1%. The sample was incubated with DAPI for 5 min, then vacuum-filtered at low pressure (100 mm Hg) and then transferred onto Waterman polycarbonate black film (25 mm outer diameter, 0.2 μm bore

diameter)^[19]. The filter film was air dried and then fixed to a glass slide with fluorescence-free immersion oil (OPTON518C) and preserved at -20°C until analysis.

1.2 APF, ANF, bacterial abundance, and biomass analysis methods

A Nikon 80i fluorescence microscope was used to observe the DAPI-stained samples. The eye lens and material lens were $10\times$ and $100\times$, respectively. Twenty fields were randomly selected for counting and for capturing images. The bacterial count and size measurement were determined using a JD801 morphological image analysis system. Abundance and biomass were calculated by a method similar to that described by Sherr et al.^[19]. The conversion factor for bacterial abundance and carbon mass was $20\text{ fg C}\cdot\text{cell}^{-1}$ ^[19], and the conversion empirical formulae for APF and ANF were as described by Menden-Deuer and Lessard^[20-21].

1.3 Data analysis

Statistical analysis of data was performed using SPSS 17.0 software. The differences in abundance of APF, ANF, and bacteria among water masses were analyzed by one-way ANOVA. Spearman correlation coefficients were used to detect correlations between environmental and biological variables.

2 Results

2.1 Sea area hydrology and nutrient distribution features

The hydrological features in the south of Herald Shoal

(170°W , 70°N) differed from those in the north (Figure 2). The sea water in the north was Bering Sea water input in winter or early spring (temperature, -1.1°C ; salinity, 33‰). The salinity feature was AW ($168^{\circ}08.73'\text{W}$ — $168^{\circ}51.98'\text{W}$, $69^{\circ}59.70'\text{N}$ — $75^{\circ}00.09'\text{N}$), in which the temperature of the upper layer was distinctly influenced by melted sea ice, and a strongly discontinuous temperature layer formed at a depth of 15—20 m (Figure 2a). In the south, the average temperature was 1°C higher and the salinity was approximately 32.5‰. These features were characteristic of BSW ($168^{\circ}59.50'\text{W}$ — $168^{\circ}51.98'\text{W}$, $69^{\circ}59.70'\text{N}$ — $65^{\circ}59.99'\text{N}$)^[5]. This was probably input water from the Bering Sea, and was influenced by local solar radiation. The surface maximum temperature was 5.8°C .

At station R00-R05 (Table 1), the salinity of the upper layer of sea water was 32.0‰—32.8‰ (Figure 2), almost the same as that at station BS12 ($168^{\circ}51.98'\text{W}$, $65^{\circ}59.99'\text{N}$). The water at BS12 was probably BSW. The melted sea ice influenced sea water in this region. The surface salinity at the Herald Shoal was low, especially at station R15 ($169^{\circ}00.40'\text{W}$, $73^{\circ}59.50'\text{N}$) and R17 ($168^{\circ}08.73'\text{W}$, $75^{\circ}00.09'\text{N}$). At station R17, the thickness of the low-salinity water layer was approximately 20 m. There were three distinctly different water masses along the surveyed transect (Figure 2b): BSW input in summer at the south of the Herald Shoal, AW input in winter or spring at the north, and surface water mixed with melted sea ice^[5].

The concentrations of phosphate, nitrate, ammonium, and chlorophyll *a* were 0.35 — $2.2\ \mu\text{mol}\cdot\text{L}^{-1}$, 0.08 — $12.71\ \mu\text{mol}\cdot\text{L}^{-1}$, 0.18 — $4.21\ \mu\text{mol}\cdot\text{L}^{-1}$, and 0.04 — $11.58\ \text{mg}\cdot\text{m}^{-3}$, respectively (Figure 3). The ratio of phosphate to nitrate was higher at station R13 than at all other stations ($P<0.05$). The nitrate concentration in the whole water column was

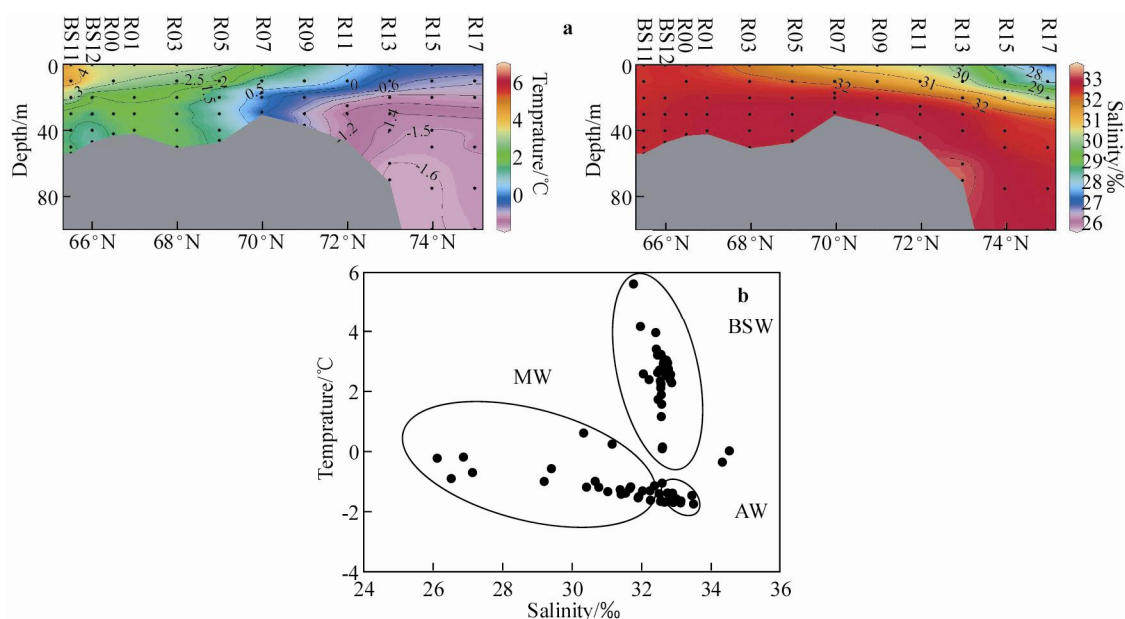


Figure 2 Temperature (T) and salinity (S) distribution in the study area: **a**, Vertical distribution of T and S; **b**, T/S Correlation diagram showing water masses: BSW=Bering Shelf Water; AW=Anadyr Water; MW=Mixed Water.

higher at R00 and R03 than at other stations. The ammonium concentration was higher at R03 than at other stations ($P<0.05$). The nitrate concentration was low at the surface layer and high at the layer below 20 m at stations R11 and R13. The ammonium concentration was lower at R15 and R17 than at all other stations ($P<0.05$). The maximum

concentration of chlorophyll *a* was at the 30 m site at station BS12 (close to Bering Strait) and the minimum was in the surface layer at station R07. Generally, the vertical distributions of nitrate and ammonium were similar along the transect, with higher concentrations in the bottom layers at stations R11, R13, and R09.

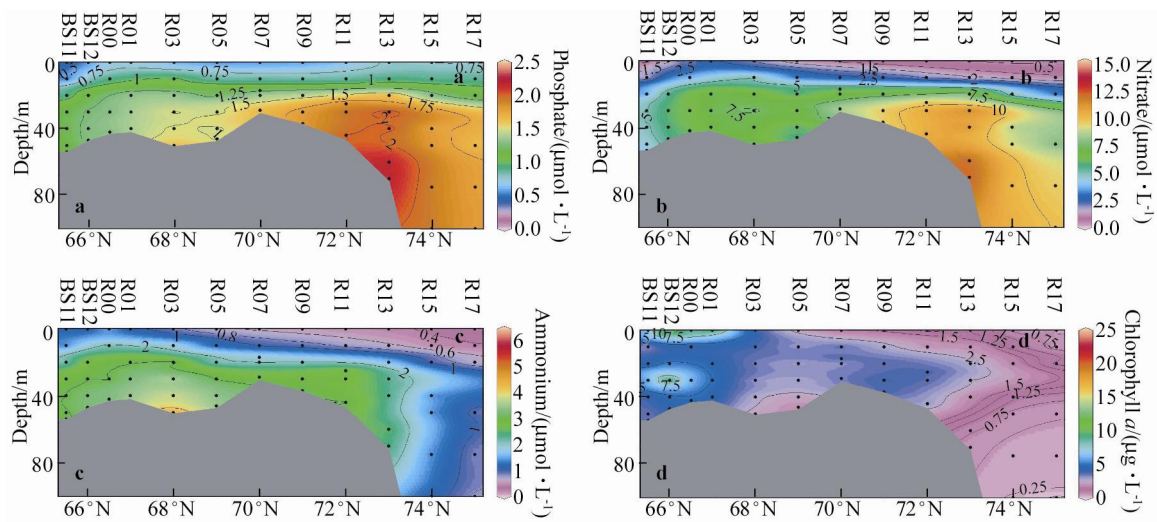


Figure 3 Vertical distribution of variables in concentrations of phosphate-phosphorus (a), nitrate-nitrogen (b), ammonium (c), and Chlorophyll *a* (d) along transect R in the Chukchi Sea.

Table 2 shows differences in concentrations of the three nutrients and chlorophyll *a* among the different water masses. The concentrations of phosphate and nitrate were higher in AW than in BSW and mixed water of melted sea

ice ($P<0.001$). The highest ammonium concentration was in BSW. The lowest concentrations of the three nutrients were in the mixed water of melted sea ice.

Table 2 Means and variation ranges of main parameters in different water masses in the Chukchi Sea

| Parameter | Water masses | | |
|--|----------------|----------------|----------------|
| | BSW | AW | MW |
| Phosphate/($\mu\text{mol}\cdot\text{L}^{-1}$) | 0.35—1.47 | 0.49—2.20 | 0.53—0.96 |
| mean | 0.96 ± 0.46 | 1.60 ± 0.51 | 0.75 ± 0.17 |
| Nitrate/($\mu\text{mol}\cdot\text{L}^{-1}$) | 0.08—9.47 | 0.24—12.71 | 0.11—0.30 |
| mean | 3.51 ± 3.68 | 7.84 ± 4.31 | 0.19 ± 0.06 |
| Ammonia/($\mu\text{mol}\cdot\text{L}^{-1}$) | 0.18—3.49 | 0.29—4.21 | 0.20—0.50 |
| mean | 1.86 ± 1.43 | 1.56 ± 2.20 | 0.36 ± 0.12 |
| Chlorophyll <i>a</i> /($\text{mg}\cdot\text{m}^{-3}$) | 0.49—11.58 | 0.04—5.80 | 0.15—3.16 |
| mean | 4.32 ± 3.92 | 1.95 ± 2.20 | 1.03 ± 1.2 |
| Bacteria/($\times 10^6$ cells· mL^{-1}) | 0.89—9.61 | 0.21—2.00 | 0.22—1.29 |
| mean | 2.67 ± 2.73 | 0.87 ± 0.61 | 0.86 ± 0.37 |
| Pico-phytoplankton/($\times 10^3$ cells· mL^{-1}) | 0.26—1.84 | 0.01—2.21 | 0.01—0.66 |
| mean | 1.03 ± 0.63 | 0.95 ± 0.77 | 0.23 ± 0.39 |
| Nano-phytoplankton/($\times 10^3$ cells· mL^{-1}) | 1.23—10.23 | 0.03—2.88 | 0.29—3.47 |
| mean | 4.56 ± 2.81 | 1.14 ± 0.84 | 1.25 ± 0.98 |

2.2 Distributions of APF and ANF

The bacterial abundance ranged from 2.10×10^5 cells·mL⁻¹ (station R17/100 m) to 9.61×10^6 cells·mL⁻¹ (station R05/30 m). There were significant differences in bacterial abundance along the whole transect ($P < 0.05$). The bacterial abundance was much higher at station R05 than at all other stations ($P < 0.001$). The lowest bacterial abundance was at station R17. The bacterial abundance showed a magnitude difference in the water mass among 0 m, 20 m, and 30 m depths at station R13.

The abundance of APF (<2 μm) ranged from 2.21×10^3 cells·mL⁻¹ (R05/10 m) to 0.01×10^3 cells·mL⁻¹ (R15/100 m) with an average of $0.74 (\pm 0.60) \times 10^3$ cells·mL⁻¹. The maximum abundance (1.02×10^4 cells·mL⁻¹) of ANF (2–20 μm) was at R05/10 m, and the minimum abundance (0.03×10^3 cells·mL⁻¹) was at R17/100 m. Most of the ANF belonged to the Centricae including *Chaetoceros socialis*, *Chaetoceros* sp. and *Thalassiosira* sp., etc. Others present included the Prymnesiophyceae, *Gymnodinium* spp., and *Dictyochaspeculum* sp.

The ANF and spatial distribution of bacteria in this region were correlated with water masses (Table 2, Figures 4 and 5). The abundances of bacteria and ANF were higher in BSW than in the other two water masses ($P < 0.05$). The APF biomass along the whole transect averaged 32% ($\pm 18\%$) of total phytoplankton (<20 μm) biomass. However, the APF biomass was 47% ($\pm 10\%$) of total phytoplankton biomass in AW, compared with 19% ($\pm 11\%$) in BSW and 19% ($\pm 11\%$) in mixed water of melted sea ice.

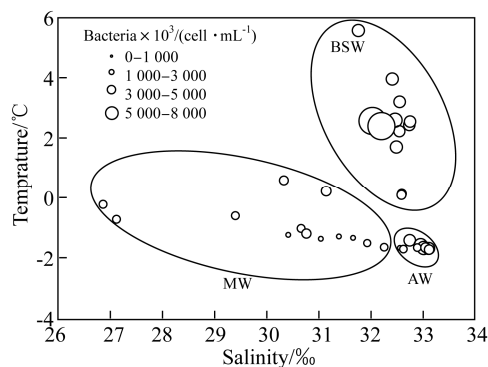


Figure 4 Distribution of bacterial abundance as a function of temperature and salinity (in different water masses): BSW=Bering Shelf Water; AW=Anadyr Water; MW=Mixed Water.

2.3 Correlations between environmental factors and APF, ANF, and bacterial abundance

Spearman correlation analysis was performed to evaluate relationships between environmental factors and APF, ANF, and bacterial abundance in each water mass (Table 3). ANF was significantly correlated with chlorophyll *a* concentration in BSW. APF was negatively correlated with ammonia and positively correlated with temperature. APF in AW was significantly correlated with chlorophyll *a* concentration,

and positively correlated with nitrate, ammonium salts, and salinity. ANF was positively correlated with chlorophyll *a* and ammonia in mixed water of melted sea ice.

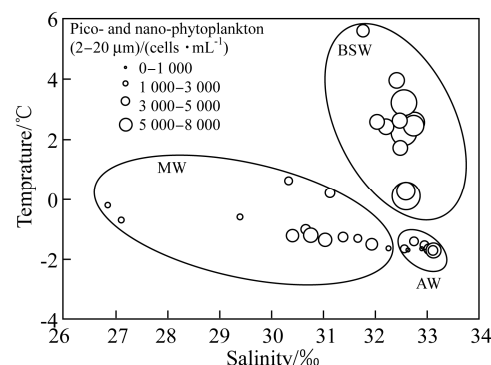


Figure 5 Distribution of pico- and nano-phytoplankton (2–20 μm) cell abundance as a function of temperature and salinity (in different water masses). BSW=Bering Shelf Water; AW=Anadyr Water; MW=Mixed Water.

Table 3 Correlation coefficients of pico- and nano-phytoplankton abundance with environmental factors in the Chukchi Sea

| | | Chlorophyll <i>a</i> | Nitrate | Ammonia | Temperature | Salinity |
|-----|-----|----------------------|---------|---------|-------------|----------|
| BSW | APF | — | — | -0.498* | 0.550* | — |
| | ANF | 0.966** | — | — | — | — |
| AW | APF | 0.976** | 0.490* | 0.833** | — | 0.472* |
| | ANF | — | — | — | — | — |
| MW | APF | — | — | — | — | — |
| | ANF | 0.878* | — | 0.941** | — | — |

Notes: **, very significant at $P < 0.001$; *, significant at $P < 0.05$.

3 Discussion

3.1 APF, ANF and bacterial abundance distribution features

In summer, Bering Sea water and coastal fresh water with a higher temperature and high salinity^[4-6,14] enter the Chukchi Sea. The abundant nutrients in both water masses provide materials for phytoplankton reproduction. Consequently, the abundance of ANF is higher in the Chukchi Sea than in any other area of the Arctic Ocean, and the abundance of APF is slightly lower than that in all other areas of the Arctic Ocean (Table 4). The very significant correlation ($P < 0.001$) between chlorophyll *a* concentration and phytoplankton abundance (<20 μm) with ANF as the major contributor ($P < 0.001$) differed from the situation in other areas of the Arctic Ocean. According to previous studies, APF abundance ranges from 70% to 88% of total phytoplankton abundance in the Mackenzie-Amundsen Shelf, North Sea, Greenland Sea, and Barents Sea^[7,22-24].

Micromonas spp. are the major components of APF, especially in the largest chlorophyll *a* layer. *Micromonas* spp. are more competitive than ANF in iceless regions with low temperatures, low nutrient concentrations, and high stratification^[25]. In comparison, warm water from the Pacific Ocean contains high levels of inorganic nutrients, especially ammonia, which promote increases in ANF in the Chukchi Sea^[26-27]. *Synechococcus* entered the Chukchi Sea along with the warm Pacific water and coastal streams. It grows rapidly in sea water with higher temperatures and high levels of DOM resulting from ANF blooms^[28]. *Synechococcus* occupies the ecological niche at the bottom of the food chain, and thus APF in the same ecological niche is restricted in a disadvantageous habitat ($P_{\text{pico-NH}_3} < 0.05$)^[25,29].

The abundance of bacterioplankton is higher in the Chukchi Sea than in any other area in the Arctic Ocean^[30-32]. The average abundance of bacterioplankton in our study was even higher than that reported for the same area in 1992^[10]. Compared with abundance data obtained by flow cytometry, those obtained using fluorescence microscopy are higher; however, the values obtained by flow cytometry are higher than those obtained using other research methods^[33]. In recent years, climate change has accelerated ice melting in the Chukchi Sea, and the rich input of coastal fresh water has seriously affected the water structure in this area. The rapid decrease of surface water restricts the vertical water exchange, and the stability of the water environment results in rapid bacterial growth^[29]. Because of the untimely melting of sea ice, more heat from solar radiation is absorbed by the ocean, phytoplankton grows more rapidly, and the DOC that is generated becomes another major factor promoting increases in bacterial abundance^[34].

The vertical distribution of ANF was almost the same as that of bacteria, and both showed maximum abundances at the bottom of the thermocline and halocline. The vertical stability in this wedge is high (Figure 6) with abundant nutrients (phosphate, nitrate and ammonium) and sufficient light, which are advantageous for phytoplankton growth.

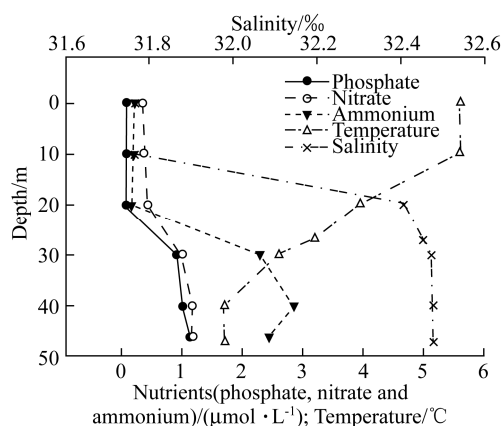


Figure 6 Profiles of temperature, salinity, and nutrients at station R05.

3.2 Correlations between ANF and bacterial distribution and Chukchi Sea water masses

In this transect, R07 is at the leading shallow beach. The temperature and salinity distribution in bottom-layer water varied between the south and north: The average temperature and salinity in the north were -1.1°C and 33‰, respectively. In this region, there is Bering Sea water input in winter or early spring, and the salinity feature is AW. The average temperature of sea water is 1°C higher in the south, and the salinity is approximately 32.5‰. As these features are characteristic of BSW, the water may be input water from the Bering Sea in the same survey period. To the north of R07, the temperature of sea water in the upper layer is affected by melted sea ice, and a strong discontinuous temperature layer forms at approximately 15–20 m^[5]. At station R05, at the south edge of the leading shallow beach, the surface temperature is high. In this area, the warm water was influenced by the shallow beach. However, likely because of geological factors, the sea water temperature in the upper layer at R07 in the north was only -0.6°C . There were two distinctly different water masses along the surveyed transect: One at the south of the leading shallow beach with BSW input in summer; and the other at the north of the leading shallow beach with AW input in winter or spring and surface water mixed with melted sea ice and the other water. This result concerning the division of water masses is the same as that obtained in the first Chinese National Arctic Research Expedition in 1999.

The abundances of bacterioplankton and ANF were higher in BSW than in the other two water masses ($P < 0.05$) (Figures 4 and 5). The results of DGGE analyses also showed that the biodiversity of bacterioplankton and ANF in BSW differed from those in the other water masses (published data unavailable). These findings indicated that the architecture of bacterioplankton and ANF communities in BSW differ from those in other water masses. In BSW, the chlorophyll *a* concentration was significantly correlated with ANF abundance ($P < 0.001$), but in AW, the chlorophyll *a* concentration was significantly correlated with APF abundance ($P < 0.001$). In summer, the solar radiation and inputs of warmer high salinity sea water from the Pacific Ocean result in the formation of open sea water and melting sea ice in the Chukchi Sea. In sea areas with sufficient sunlight and high nutrients, the ANF community is more competitive than the APF community^[35]. Therefore, the effect of Pacific input water in summer is to replace the local phytoplankton community in the Chukchi Sea with a foreign phytoplankton community. Such community succession may transform the Chukchi Sea summer ecosystem into an ecotone. The resistance against foreign interference and system stability will be weakened, while sensitivity to ecological change will be increased. As a result, some unhealthy red tides that usually occur in humid tropical sea areas can break out in summer in the Chukchi Sea^[36-37]. In conclusion, the Pacific Ocean brings not only warmer and

higher salinity water to the Chukchi Sea in summer, it also brings many foreign species and further influences micro-organism architecture.

Acknowledgements We thank Prof. Zhao Jinping, Ocean University of China, for providing hydrological data for the Chukchi Sea from the 3rd CHINARE-Arctic. We also thank Prof. Chen Jianfang, the Second Institute of Oceanography, SOA, for providing nutrient data. This study was financially supported by the National Natural Science Foundation of China (Grant no. 41076130). Sample information and data were provided by the Resource-sharing Platform of Polar Samples (<http://birds.chinare.org.cn>) maintained by the Polar Research Institute of China (PRIC) and the Chinese National Arctic & Antarctic Data Center (CN-NADC).

References

- Wang H W, Chen H X, Lu L G, et al. Study of tide and residual current observations in Chukchi Sea in the summer 2008. *Acta Oceanologica Sinica*, 2011, 33(6): 1-8 (in Chinese).
- Aagaard K, Coachman L K, Carmack E C. On the halocline of the Arctic Ocean. *Deep-Sea Res*, 1981, 28(6): 529-545.
- Coachman L K, Aagaard K. *Physical oceanography of Arctic and Subarctic Seas*. New York: Springer-Verlag, 1974: 1-72.
- Tang Y X, Jiao Y T, Zou E M. A preliminary analysis of the hydrographic features and water masses in the Bering Sea and the Chukchi Sea. *Chinese Journal of Polar Research*, 2001, 13: 57-68. (in Chinese)
- Zhao J P, Shi J X, Jin M M, et al. Water mass structure of the Chukchi Sea during ice melting period in the Summer of 1999. *Adv Earth Sci*, 2010, 25(2): 154-162 (in Chinese).
- Garneau M È, Vincent W F, Alonso-Sáez L, et al. Prokaryotic community structure and heterotrophic production in a river-influenced coastal Arctic ecosystem. *Aqua Microb Ecol*, 2006, 42(1): 27-40.
- Schloss I R, Nozais C, Mas S, et al. Picophytoplankton and nanophytoplankton abundance and distribution in the southeastern Beaufort Sea (Mackenzie Shelf and Amundsen Gulf) during Fall 2002. *J Mar Syst*, 2008, 74(3-4): 978-993.
- Sambrotto R N, Goering J J, McRoy C P. Large yearly production of phytoplankton in the Western bering strait. *Science*, 1984, 255(4667): 1147-1150.
- Liu Z L, Chen J F, Zhang T, et al. Size-fractionated chlorophyll *a* and primary productivity in the Chukchi Sea and its northern Chukchi Plateau. *Acta Ecologica Sinica*, 2007, 27(12): 4953-4962.
- Steward G F, Smith D C, Azam F. Abundance and production of bacteria and viruses in the Bering and Chukchi Seas. *Mar Ecol Prog Ser*, 1996, 131: 287-300.
- Wheeler P A, Gosselin M, Sherr E, et al. Active cycling of organic carbon in the central Arctic Ocean. *Nature*, 1996, 380(6576): 697-699.
- Gosselin M, Levasseur M, Wheeler P A, et al. New measurements of phytoplankton and ice algal production in the Arctic Ocean. *Deep-Sea Res II*, 1997, 44(8): 1623-1644.
- Sherr E B, Sherr B F, Wheeler P A, et al. Temporal and spatial variation in stocks of autotrophic and heterotrophic microbes in the upper water column of the central Arctic Ocean. *Deep-Sea Res*, 2003, 50(5): 557-571.
- Cota G F, Pomeroy L R, Harrison W G, et al. Nutrients, primary production and microbial heterotrophy in the southeastern Chukchi Sea: Arctic summer nutrient depletion and heterotrophy. *Mar Ecol Prog Ser*, 1996, 135: 247-258.
- Hill V, Cota G, Stockwell D. Spring and summer phytoplankton communities in the Chukchi and Eastern Beaufort Seas. *Deep-Sea Res II*, 2005, 52(24-26): 3369-3385.
- Kirchman D L, Hill V, Cottrell M T, et al. Standing stocks, production, and respiration of phytoplankton and heterotrophic bacteria in the western Arctic Ocean. *Deep-Sea Res II*, 2009, 56(17): 1237-1248.
- Li H L, Chen J F, Gao S Q, et al. Nutrients variation of the Pacific inflow in the western Arctic Ocean. *Acta Oceanologica Sinica*, 2011, 33(2): 85-95.
- Parsons T R, Maits Y, Lalli C M. *A Manual of Chemical and Biological Methods for Seawater Analysis*. Oxford: Pergamon Press, 1984: 101-173.
- Sherr E B, Sherr B F, Fessenden L. Heterotrophic protists in the Central Arctic Ocean. *Deep-Sea Res II*, 1997, 44(8): 1665-1682.
- Menden-Deuer S, Lessard E J. Carbon to volume relationships for dinoflagellates, diatoms, and other protist plankton. *Limnol Oceanogr*, 2000, 45(3): 569-579.
- Wang G Z, Guo C Y, Luo W, et al. The distribution of picoplankton and nanoplankton in Kongsfjorden, Svalbard during late summer 2006. *Polar Biol*, 2009, 32(8): 1233-1238.
- Mostajir B, Gosselin M, Gratton Y, et al. Surface water distribution of pico- and nanophytoplankton in relation to two distinctive water masses in the North Water, northern Baffin Bay, during fall. *Aquat Microb Ecol*, 2001, 23(2): 205-212.
- Booth B C, Smith W O Jr. Autotrophic flagellates and diatoms in the Northeast Water polynya, Greenland: summer 1993. *J Mar Syst*, 1997, 10(1-4): 241-261.
- Not F, Ramon M, Mikel L, et al. Late summer community composition and abundance of photosynthetic picoeukaryotes in Norwegian and Barents Seas. *Limnol Oceanogr*, 2005, 50(5): 1677-1686.
- Li W K W, McLaughlin F A, Lovejoy C, et al. Smallest algae thrive as the Arctic Ocean freshens. *Science*, 2009, 326(5952): 539.
- Carmack E C, MacDonald R W. Oceanography of the Canadian shelf of the Beaufort Sea: a setting for marine life. *Arctic*, 2002, 55(S1): 29-45.
- Lovejoy C, Massana R, Pedrós-Alió C. Diversity and distribution of marine microbial eukaryotes in the Arctic Ocean and adjacent seas. *Appl Environ Microb*, 2006, 72(5): 3085-3095.
- Cottrell M T, Kirchman D L. Photoheterotrophic microbes in the Arctic Ocean in summer and winter. *Appl Environ Microbiol*, 2009, 75(15): 4958-4966.
- Vincent W F. Microbial ecosystem responses to rapid climate change in the Arctic. *ISME J*, 2010, 4(9): 1087-1090.
- Rich J, Gosselin M, Sherr E, et al. High bacterial production, uptake and concentrations of dissolved organic matter in the Central Arctic Ocean. *Deep-Sea Res II*, 1997, 44(8): 1645-1663.
- Wells L E, Deming J W. Abundance of bacteria, the Cytophaga-Flavobacterium cluster and archaea in cold oligotrophic waters and nepheloid layers of the Northwest Passage, Canadian Archipelago. *Aquat Microb Ecol*, 2003, 31(1): 19-31.
- Meon B, Amon R M W. Heterotrophic bacterial activity and fluxes of dissolved free amino acids and glucose in the Arctic river Ob, Yenisei and the adjacent Kara Sea. *Aquat Microb Ecol*, 2004, 37(2): 121-135.
- Lin L, He J F, Zhang F, et al. Heterotrophic bacterial abundance and distribution in the Bering Sea and the Arctic Ocean in the summer of 2008. *Acta Oceanologica Sinica*, 2011, 33(2): 166-174.
- Kirchman D L, Morán X A G, Ducklow H. Microbial growth in the polar oceans—role of temperature and potential impact of climate change. *Nat Rev Microbiol*, 2009, 7(6): 451-459.
- Parsons T R, Takahashi M. Environmental control of phytoplankton cell size. *Limnol Oceanogr*, 1973, 18(4): 511-515.
- Vincent W F, Whyte L G, Lovejoy C, et al. Arctic microbial ecosystems and impacts of extreme warming during the International Polar Year. *Polar Sci*, 2009, 3(3): 171-180.
- Eilertsen H C, Degerlund M. Phytoplankton and light during the northern high-latitude winter. *J Plankt Res*, 2010, 32(6): 899-912.